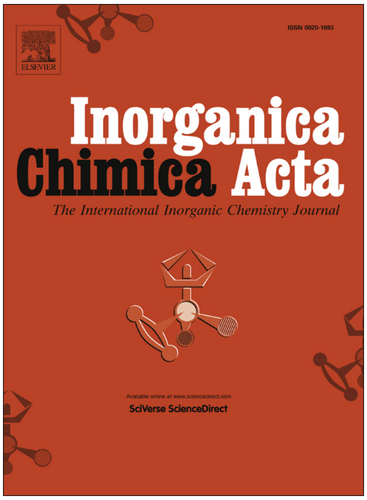

Redox properties of cobalt(II) complexes with azole-pyridines

Nail M. Shavaleev, Florian Kessler, Michael Grätzel, Mohammad K. Nazeeruddin

PII: S0020-1693(13)00437-4
DOI: http://dx.doi.org/10.1016/j.ica.2013.07.057
Reference: ICA 15600

To appear in: *Inorganica Chimica Acta*

Received Date: 24 June 2013
Revised Date: 30 July 2013
Accepted Date: 31 July 2013

Please cite this article as: N.M. Shavaleev, F. Kessler, M. Grätzel, M.K. Nazeeruddin, Redox properties of cobalt(II) complexes with azole-pyridines, *Inorganica Chimica Acta* (2013), doi: http://dx.doi.org/10.1016/j.ica.2013.07.057

Redox properties of cobalt(II) complexes with azole-pyridines

Nail M. Shavaleev [a,]*, Florian Kessler[a,b], Michael Grätzel[a], Mohammad K. Nazeeruddin[a,]*

[a]*Laboratory of Photonics and Interfaces, École Polytechnique Fédérale de Lausanne, CH-1015 Lausanne, Switzerland.*

[b]*Present address: Siemens AG, Corporate Technology, CT RTC MAT MPV, Günther-Scharowsky Strasse 1, D-91058 Erlangen, Germany.*

*Corresponding authors. Tel.: +41 21 693 6124; fax: +41 21 693 4111. *E-mail addresses:* shava@mail.ru (N.M. Shavaleev), mdkhaja.nazeeruddin@epfl.ch (M.K. Nazeeruddin).

Keywords: Azole; Ligand; Cobalt; Complex; Electrochemistry; Voltammetry

Highlights

>Five new bidentate and tridentate azole-pyridine ligands.

>Nine new homoleptic octahedral cobalt(II) complexes with azole-pyridines.

>How to control redox and optical properties of cobalt(II) complexes.

Graphical Abstract

Redox and optical properties of homoleptic octahedral cobalt(II) complexes with bidentate and tridentate azole-pyridine ligands.

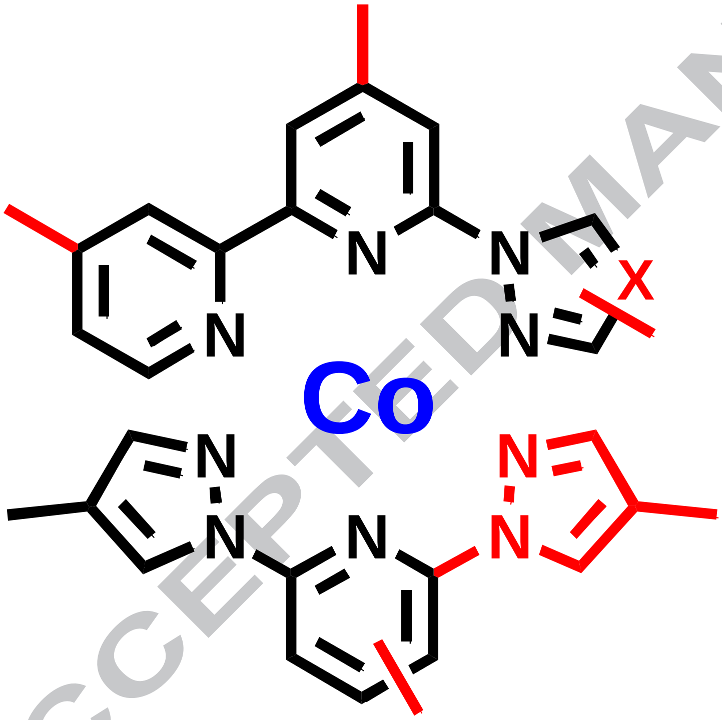

Abstract

We report nine new homoleptic octahedral cobalt(II) complexes $[Co(N^{\wedge}N)_3]^{2+}$ and $[Co(N^{\wedge}N^{\wedge}N)_2]^{2+}$ with bidentate or tridentate azole-pyridine ligands (where azole is 1,2,4-triazole or a substituted pyrazole). The complexes are air- and moisture-stable solids of pale pink to pale brown color that exhibit quasi-reversible redox processes in polar organic solvents. By changing azole heterocycle and by adding methyl groups, we tune redox potentials of the complexes from 0.05 V to 0.5 V for the Co(III/II) couple (its cyclic voltammogram depends on the electrode history) and from −1.08 V to −1.57 V for the Co(II/I) couple to give a redox gap of 1.37–1.82 V. Replacing a pyrazole with electron-deficient 1,2,4-triazole strongly positively shifts redox potentials of the complexes; in contrast, adding electron-donor methyl groups shifts the potentials negatively.

1. Introduction

Redox processes in cobalt polypyridyl complexes give access to Co(III/II/I) metal oxidation states and to reduced coordinated ligand(s) [1–10]. Cobalt polypyridyl complexes are used as redox catalysts for electro-reduction/oxidation of carbon dioxide, oxygen and water [11–15]; as redox shuttles [16–20] and p-dopants [21] for dye-sensitized solar cells; and as electrochemical energy storage materials for batteries [22]. These applications are likely to be developed further because cobalt is an abundant element [11], but to do that, one has to have control over redox properties of its complexes.

Easy-to-make azole ligands are used to replace/complement polypyridyls in coordination chemistry [23–35], but few studies have investigated cobalt–azole complexes [36–40]. Here, we report synthesis and electrochemistry of nine new octahedral cobalt(II) complexes with bidentate or tridentate azole-pyridine ligands (Scheme 1).

2. Results and discussion

2.1. Synthesis and characterization

The azole-pyridine ligands **L1**–**L9** were prepared by non-catalyzed C–N coupling of an azole with fluoro-, chloro- or bromo-pyridine in DMSO, in the presence of potassium tert-butoxide as a base (Scheme 1) [31,41]. Ligands **L2** and **L6**–**L9** are new. **L1** was reported by us before [31]. **L3**–**L5** were reported [32–35], but we have made their synthesis faster and more user-friendly. With 1,2,4-triazole, only the major product was isolated, the N1/N2-derivative **L6** and **L9**.

Electron-donor methyl groups were added to **L1**–**L9** to make the ligand more electron-rich to increase its affinity to cobalt, and to improve solubility and change redox properties of its cobalt complexes.

Nine new homoleptic octahedral cobalt(II) complexes **1**–**9** were prepared as hexafluorophosphate salts by the reaction of $CoCl_2 \cdot 6H_2O$ with an excess of ligand **L1**–**L9** in hot methanol and by the anion exchange with KPF_6 (Scheme 1). **1**–**9** are air- and moisture-stable pale pink to pale brown solids that are soluble in polar organic solvents. **1**–**9** were characterized by C, H, N elemental analysis; their ESI^+ TOF mass-spectra exhibit peaks of the cations $\{M - PF_6\}^+$ and $\{M - 2PF_6\}^{2+}$.

NMR spectra of **1**–**9** are solvent-independent in acetone-d_6 and acetonitrile-d_3 (Supplementary material). Because cobalt(II) is paramagnetic [20,42], ^{1}H NMR signals of **1**–**9** are observed in a wide chemical-shift range. ^{1}H NMR spectra of **1** and **2** are broad because of fast fac-mer isomerisation of non-symmetric bidentate ligands **L1** and **L2** at labile Co(II) ion [43]. In contrast, ^{1}H NMR spectra of complexes **3**–**9** with tridentate ligands exhibit sharp singlets and confirm C_2 symmetry of **3**–**9**. ^{19}F NMR spectra of **1**–**9** confirm the presence of PF_6^- anions that are not bound to Co(II).

Outward-facing N4-atom in 1,2,4-triazole of ligands **L6** and **L9** does not interfere with the synthesis of mono-nuclear complexes $[Co(N\text{^}N\text{^}N)_2]^{2+}$, **6** and **9**, that is, it does not give rise to coordination polymers. Sterically-hindering 3,5-dimethyl groups in the pyrazole of ligands **L5** and **L8** do not interfere with the synthesis of complexes **5** and **8**.

2.2. Absorption spectroscopy

Ligands **L1**–**L9** give colorless solutions in organic solvents. For **L1**–**L9**, we observe a long-wavelength absorption shoulder in dichloromethane that is absent in acetonitrile and that may originate from an azole-to-pyridine charge-transfer transition (Tables 1 and S3 and Fig. S7–S15).

Complexes **1**–**9** give colorless or pale yellow solutions in dichloromethane and in acetonitrile. Electronic absorption spectra of **1**–**9** are solvent-independent (Tables 1 and S3 and Fig. 1 and S16–S24); therefore, we consider that the coordination environment around cobalt(II) is the same in dichloromethane and in acetonitrile (recall that NMR spectra of **1**–**9** are solvent-independent too, Supplementary material). In the visible range, absorption spectra of **1**–**9** exhibit a shoulder that goes up to 500 nm with molar absorption coefficients of $\leq 10^3$ M^{-1} cm^{-1} at $\lambda > 400$ nm (Table 1 and Fig. 1).

Electronic absorption spectra of the ligands and their cobalt(II) complexes exhibit a small red-shift from acetonitrile to dichloromethane; a large red-shift and a gain in intensity when a conjugated π-system increases from bidentate to tridentate ligands; but a blue-shift when electron-donor methyl groups are added to the 4,4′-positions of the 2,2′-bipyridine and/or when a pyrazole is replaced by electron-deficient 1,2,4-triazole to destabilize azole-to-pyridine charge-transfer transition (Tables 1 and S3 and Fig. S7–S24).

2.3. Electrochemistry

The redox potentials of cobalt(II) complexes **1**–**9** were measured with cyclic voltammetry on gold and on glassy-carbon electrodes in acetonitrile (ACN) and in DMF and are reported relative to ferrocene couple [44] (Tables 2, S1 and S2 and Fig. 2–4 and S1–S6). The one-electron redox processes of **1**–**9** were assigned by comparison with the literature [1–10]. In cyclic voltammograms (CV) of **1**–**9**, we observe Co(III/II) oxidation and Co(II/I) reduction, followed by reduction(s) of the coordinated ligand(s) L/L^- [1–10]. Redox processes in **1**–**9** are quasi-reversible with peak-to-peak separation that is larger than that for the ferrocene and that increases at faster scan rates, indicating a slow electron-transfer for **1**–**9** on the electrode (Tables 2, S1 and S2). Redox potentials of **1**–**9** do not depend on the electrode material and vary only by ≤50 mV within the scan-rate range of 0.05–5 V/s; however, Co(II/I) and L/L^{-} couples exhibit higher reversibility (smaller peak-to-peak separation) on glassy-carbon electrode, while Co(III/II)—on gold (Tables 2, S1 and S2 and Fig. 2, 3 and S1–S6). Others have previously noted too that the reversibility of Co(III/II) couple depends on the electrode material [10,17].

The redox processes of **1**–**9** become more reversible from DMF to ACN; from bidentate to tridentate ligands (complexes with higher denticity ligands often have higher electrochemical stability); from 2,6-bis-azole-pyridine to 6-azole-2,2′-bipyridines (azoles are weaker ligands than pyridines are [23,25,38]); and from 1,2,4-triazole to pyrazole ligands (1,2,4-triazole may interact with the electrode through the N4-atom) (Tables 2, S1 and S2). The redox potential of the Co(II/I) couple in **1** and **2** and that of the Co(III/II) couple in **4** and **5** becomes less positive by ≤100 mV from ACN to DMF, indicating that the solvent interacts to some extent with the cobalt (Tables S1 and S2).

In the complexes with bidentate ligands (**1** and **2**), the reduction that follows Co(II/I) couple can be a two-electron process [1,2], but because it is irreversible, we do not discuss it. In the complexes with tridentate ligands (**3**–**9**), one-electron ligand-centered L/L^{-} reductions that follow Co(II/I) couple [1–10] are quasi-reversible at fast scan rate (1 V/s), but are often irreversible at slow scan rate (0.1 V/s), indicating that these electrochemical processes are accompanied by chemical reactions, for example, octahedral Co(I) complexes [5,6] can eject coordinated ligands [1,2,8].

In **1**–**9**, cyclic voltammogram of the Co(III/II) couple depends on the electrode history, that is, it is quasi-reversible and reproducible only when the potential stays sufficiently positive to avoid Co(II/I) reduction. After cycling the potential to the negative range beyond the Co(II/I) couple, on return scan, CV of the Co(III/II) couple becomes irreproducible and broad and its current decreases (Fig. 4). We conclude that the Co(II/I) couple produces 'reduced Co species' that adsorb on the electrode and passivate it towards the Co(III/II) couple (recall that all redox processes in **1**–**9** are quasi-reversible). The electrode can be reactivated by multiple cycling of the potential in the positive range or by mechanical cleaning. In contrast, cyclic voltammograms of the Co(II/I) and L/L^- couples in **1**–**9** do not depend on the electrode history (Fig. 4).

Cyclic voltammogram of the Co(III/II) couple in **1**–**9** is often non-symmetric with a broad Co(II)→Co(III) wave, especially on a glassy-carbon electrode, but a narrow Co(III)→Co(II) wave (Fig. 2 and 3). In octahedral polypyridyl complexes, Co(II), a d^7 ion, is usually high-spin, $t_{2g}^5e_{2g}^2$, the contribution of low-spin $t_{2g}^6e_{2g}^1$ component depends on the environment (we did not investigate magnetism of **1**–**9**); in contrast, Co(III), a d^6 ion, is low-spin, $t_{2g}^6e_{2g}^0$ [20,42]. A spin change required by the Co(III/II) couple may cause non-symmetric CV of **1**–**9** [10,17].

In acetonitrile, on Pt/FTO electrode, non-substituted analog of **1** and **2**, reference complex **R1** (Chart 1), exhibits $E_{1/2}^{ox}$ = 0.32 V and $E_{1/2}^{red}$ = −1.45 V [19], while non-substituted analog of **4**, **5**, **7** and **8**, reference complex **R2** (Chart 1), exhibits $E_{1/2}^{ox}$ = 0.22 V and $E_{1/2}^{red}$ = −1.20 V [19]. It is clear, from comparison of **R1** and **R2** with the new complexes, that by adding electron-donor methyl groups to the ligand we make it stronger σ-donor and weaker π-acceptor, and we negatively shift redox potentials of its cobalt complex by ≤170 mV (Table 2).

By replacing 4-methylpyrazole (**4**, **7**) with more electron-rich 3,5-dimethylpyrazole (**5**, **8**), we negatively shift redox potentials of the complexes by ≤60 mV (Table 2). By replacing 2,2′-bipyridyl in **4**–**6** with more electron-rich 4,4′-dimethyl-2,2′-bipyridyl in **7**–**9**, we negatively shift $E_{1/2}^{ox}$ by ≤80 mV and $E_{1/2}^{red}$ by ≤120 mV (Table 2). In contrast, by replacing pyrazole (**R2**, **4**, **5**, **7**, **8**) with electron-deficient 1,2,4-triazole (**6**, **9**), we strongly positively shift $E_{1/2}^{\mathrm{ox}}$ by ≤340 mV and $E_{1/2}^{\mathrm{red}}$ by ≤180 mV (Table 2).

In metal complexes, neutral azoles are weaker σ-donors/π-acceptors and, therefore, weaker ligands than pyridines are [23,25,38] that explains the trends in redox potentials and the often irreversible electrochemistry observed for **1**–**9** (Table 2). Others have previously noted too that the Co(III/II) couple in $[\mathrm{Co(N^\wedge N^\wedge N)_2}]^{2+}$ complexes became less reversible and its potential shifted positively when the pyridines in 2,2′;6′,2″-terpyridine were replaced by pyrazoles [38].

We change redox potentials of complexes **1**–**9** from 0.05 V to 0.5 V for the Co(III/II) couple, from −1.08 V to −1.57 V for the Co(II/I) couple, and from −2.04 V to −2.14 V for the L/L^{-} couple (Table 2). The potential of the Co(III/II) couple (oxidation) increases when there are more of weak σ-donor pyrazoles and less of strong σ-donor pyridines coordinated to cobalt(II) from **4**, **5**, **7** and **8** (2 pyrazoles and 4 pyridines per Co, $E_{1/2}^{\mathrm{ox}}$ of 0.05–0.17 V) to **1** and **2** (3 pyrazoles and 3 pyridines per Co, 0.19–0.21 V) and to **3** (4 pyrazoles and 2 pyridines per Co, 0.50 V). The potential of the Co(II/I) couple (first reduction) is largely determined by π-acceptor strength of the ligand and increases from bidentate ligands (**1** and **2**, $E_{1/2}^{\mathrm{red}}$ of −1.53 V to −1.57 V) to stronger π-acceptor tridentate ligands (**3**–**9**, −1.08 V to −1.37 V) and from pyrazole ligands (**4**, **5**, **7** and **8**, −1.24 V to −1.37 V) to more electron-deficient and stronger π-acceptor 1,2,4-triazole ligands (**6** and **9**, −1.08 V to −1.19 V). The potential of the L/L^{-} couple (second reduction for **4**, **5**, **7** and **8**) shifts negatively by 10–40 mV when 4-methylpyrazole (**4**, **7**) is replaced by more electron-rich 3,5-dimethylpyrazole (**5**, **8**) and by 60–90 mV when 2,2′-bipyridyl (**4, 5**) is replaced by more electron-rich 4,4′-dimethyl-2,2′-bipyridyl (**7**, **8**).

Redox gap of the complex, $\Delta E = E_{1/2}^{\mathrm{ox}}$ [Co(III/II)] − $E_{1/2}^{\mathrm{red}}$ [Co(II/I)], increases (i) when there are more of weak σ-donor/π-acceptor azoles and less of strong σ-donor/π-acceptor pyridines coordinated to the cobalt from **4**–**9** (2 azoles and 4 pyridines per Co, Δ*E* of 1.37–1.58 V) to **1** and **2** (3 azoles and 3 pyridines per Co, 1.76 V) and to **3** (4 azoles and 2 pyridines per Co, 1.82 V) and (ii) when a pyrazole is replaced by 1,2,4-triazole from **4**, **5**, **7** and **8** (1.37–1.45 V) to **6** and **9** (1.51–1.58 V) (Table 2).

3. Conclusions

We control optical and redox properties of cobalt(II) complexes **1**–**9** with bidentate and tridentate azole-pyridines by changing azole heterocycles and by adding methyl groups. **1**–**9** do not have strong optical transitions (are transparent) in the visible range. **4**, **5**, **7** and **8** have low Co(III/II) potentials of 0.05–0.17 V and can be used as redox shuttles in dye-sensitized solar cells [16–20]. **3**, **6** and **9** have high Co(III/II) potentials of 0.37–0.50 V and can be applied, in the Co(III) oxidation state, as p-dopants [21] for organic electronics and as oxidizers. Electron-deficient 1,2,4-triazole strongly positively shifts redox potentials of cobalt complexes.

One can incorporate azole heterocycles in polydentate [14,15] and bridging [36,45–48] ligands for cobalt; for example, cobalt complexes with quadridentate [14] and pentadentate [15] ligands and hetero-polynuclear cobalt–ruthenium [47] and cobalt–iridium [48] complexes find use in electrical/solar-to-chemical energy conversion. One can coordinate easy-to-make azole-pyridines **L1**–**L9** and their analogs to a variety of *d*- and *f*-metals [23–35].

4. Experimental

Purification and handling of all compounds were carried out under air. All products were stored in the dark. Chemicals from commercial suppliers were used without purification.

Chromatography was performed on a column with an i.d. of 30 mm on silica gel 60 (Fluka, Nr 60752) or on silica gel (ultra pure, 40-60 µm, 60A; Acros, Nr 36005). The progress of reactions and the elution of products were followed on TLC plates (silica gel 60 F_{254} on aluminum sheets, Merck).

Elemental analyses were performed by Dr. E. Solari, Service for Elemental Analysis, Institute of Chemical Sciences and Engineering (ISIC EPFL). ^{1}H, ^{13}C, and ^{19}F NMR spectra were recorded with AV400 and AVIII-400 spectrometers (400 MHz, Bruker). Mass spectra were recorded with Q-TOF Ultima (Waters) and TSQ7000 (Thermo Fisher) spectrometers (Mass-Spectroscopy Service, ISIC EPFL).

Electronic absorption spectra were recorded with an HP/Agilent 8453 Diode Array UV/VIS spectrophotometer under air in optical cells of 2 or 10 mm path length. The solutions in CH_2Cl_2 (Sigma-Aldrich, puriss p.a., ACS reagent) or acetonitrile (Fisher Scientific, Far UV, HPLC Gradient Grade) were freshly prepared before experiment.

4.1. Synthesis of ligands

The structures of **L1**–**L9** are shown in Scheme 1. The synthesis of **L1** was reported by us before [31]. The reaction was performed under argon. Substituted azole (excess) and potassium tert-butoxide (^{t}BuOK excess, Acros) were dissolved at RT in dry and degassed DMSO (3.5–4 mL, Acros, 99.8%, ExtraDry, over Molecular Sieves, AcroSeal$^{®}$). An exothermic reaction occurred. The mixture was stirred for 10 min to allow the reaction to finish and cool. Then, a substituted halopyridine was added. The reaction mixture was stirred for 24 h at either 110 °C (**L2**) or 140 °C (**L3**–**L9**) to give a suspension ranging in colour from white to dark-red. It was cooled to RT. Water (50 mL) was added: the product precipitated as solid or as oil that solidified on stirring/sonication. The solid was filtered, washed with water, and extracted with ether and water (**L2**) or with dichloromethane and water (**L3**–**L9**). The organic layer was washed with water to extract DMSO. Purification by chromatography on silica (20 g) removed the starting materials and by-products on elution with 0–0.4% CH_3OH in CH_2Cl_2, and provided the pure product on elution with 0.4–1.0 % CH_3OH in CH_2Cl_2. Further details are provided below.

L2: 4-Methylpyrazole (0.9 mL, 0.89 g, 10.8 mmol, Acros), ^{t}BuOK (1.21 g, 10.8 mmol), and 2-fluoro-5-methylpyridine (1 g, 9.0 mmol, Acros) gave white crystalline solid: 1.26 g (7.3 mmol, 81%). *Anal.* Calc. for $C_{10}H_{11}N_3$ (MW 173.21): C, 69.34; H, 6.40; N, 24.26. Found: C, 69.99; H, 6.24; N, 24.89%. ^{1}H NMR (400 MHz, $CDCl_3$): δ = 8.29 (s, 1H), 8.20 (s, 1H), 7.82 (d, J = 8.4 Hz, 1H), 7.61 (d, J = 8.0 Hz, 1H), 7.53 (s, 1H), 2.35 (s, 3H, CH_3), 2.17 (s, 3H, CH_3) ppm. ^{13}C NMR (100 MHz, $CDCl_3$): δ = 150.0, 148.0, 142.7, 139.3, 130.6, 125.5, 118.3, 111.7, 18.0, 9.2 ppm. ESI$^+$ MS: *m/z* 174.2 ($\{M + H\}^+$, 100%).

L3: 4-Methylpyrazole (1.68 mL, 1.66 g, 20 mmol, Acros), ^{t}BuOK (2.27 g, 20 mmol), and 2,6-dichloropyridine (1 g, 6.8 mmol, Aldrich) gave white solid: 1.12 g (4.7 mmol, 69%). *Anal.* Calc. for $C_{13}H_{13}N_5$ (MW 239.28): C, 65.25; H, 5.48; N, 29.27. Found: C, 65.04; H, 5.51; N, 29.87%. ^{1}H NMR (400 MHz, $CDCl_3$): δ = 8.35 (s, 2H), 7.89 (t, J = 8.0 Hz, 1H), 7.76 (d, J = 8.0 Hz, 2H), 7.58 (s, 2H), 2.20 (s, 6H, CH_3) ppm. ^{13}C NMR (100 MHz, $CDCl_3$): δ = 150.2, 143.5, 141.3, 125.6, 118.7, 108.6, 9.2 ppm. ESI$^+$ MS: *m/z* 240.3 ($\{M + H\}^+$, 100%), 262.2 ($\{M + Na\}^+$, 16%).

L4: 4-Methylpyrazole (0.53 mL, 0.52 g, 6.3 mmol, Acros), ^{t}BuOK (0.72 g, 6.4 mmol), and 6-bromo-2,2'-bipyridine (1 g, 4.3 mmol, ABCR) gave white solid: 0.92 g (3.9 mmol, 91%). *Anal.* Calc. for $C_{14}H_{12}N_4$ (MW 236.27): C, 71.17; H, 5.12; N, 23.71. Found: C, 71.44; H, 5.10; N, 24.05%. ^{1}H NMR (400 MHz, $CDCl_3$): δ = 8.71 (d, J = 4.4 Hz, 1H), 8.51 (s, 1H), 8.48 (d, J = 8.0 Hz, 1H), 8.29 (dd, J = 7.2, 1.2, 1H), 8.00–7.90 (m, 2H), 7.86 (td, J = 7.6, 1.6, 1H), 7.59 (s, 1H), 7.35 (dd, J = 6.8, 5.2 Hz, 1H), 2.21 (s, 3H, CH_3) ppm. ^{13}C NMR (100 MHz,

$CDCl_3$): δ = 155.6, 154.6, 151.2, 149.4, 143.2, 139.7, 137.0, 125.6, 124.1, 121.3, 118.5, 118.2, 112.2, 9.3 ppm. ESI$^+$ MS: *m/z* 237.3 ({M + H}$^+$, 100%), 259.2 ({M + Na}$^+$, 8%).

L5: 3,5-Dimethylpyrazole (0.61 g, 6.3 mmol, Fluka), ^{t}BuOK (0.72 g, 6.4 mmol), and 6-bromo-2,2'-bipyridine (1 g, 4.3 mmol, ABCR) gave pale-yellow solid: 0.82 g (3.3 mmol, 76%). *Anal.* Calc. for $C_{15}H_{14}N_4$ (MW 250.30): C, 71.98; H, 5.64; N, 22.38. Found: C, 72.04; H, 5.48; N, 22.48%. ^{1}H NMR (400 MHz, $CDCl_3$): δ = 8.71 (d, *J* = 4.4 Hz, 1H), 8.37 (d, *J* = 8.0 Hz, 1H), 8.38–8.30 (br, 1H), 7.97–7.90 (m, 2H), 7.86 (t, *J* = 7.6 Hz, 1H), 7.40–7.31 (m, 1H), 6.05 (s, 1H), 2.81 (s, 3H, CH_3), 2.34 (s, 3H, CH_3) ppm. ^{13}C NMR (100 MHz, $CDCl_3$): δ = 155.9, 154.3, 153.2, 150.0, 149.4, 141.5, 139.5, 137.1, 124.0, 121.2, 117.9, 115.8, 103.4, 15.4, 13.9 ppm. ESI$^+$ MS: *m/z* 251.1 ({M + H}$^+$, 100%), 273.1 ({M + Na}$^+$, 12%).

L6: 1,2,4-Triazole (0.44 g, 6.4 mmol, Aldrich), ^{t}BuOK (0.72 g, 6.4 mmol), and 6-bromo-2,2'-bipyridine (1 g, 4.3 mmol, ABCR) gave white solid: 0.57 g (2.6 mmol, 60%). *Anal.* Calc. for $C_{12}H_9N_5$ (MW 223.23): C, 64.56; H, 4.06; N, 31.37. Found: C, 64.13; H, 3.96; N, 32.08%. ^{1}H NMR (400 MHz, $CDCl_3$): δ = 9.33 (s, 1H), 8.73 (d, *J* = 4.4 Hz, 1H), 8.50–8.42 (m, 2H), 8.15 (s, 1H), 8.04 (t, *J* = 8.0 Hz, 1H), 7.95 (d, *J* = 8.0 Hz, 1H), 7.90 (td, *J* = 8.0, 1.6 Hz, 1H), 7.39 (dd, *J* = 6.4, 4.8 Hz, 1H) ppm. ^{13}C NMR (100 MHz, $CDCl_3$): δ = 155.3, 154.8, 153.1, 149.5, 149.0, 141.6, 140.4, 137.2, 124.5, 121.3, 120.4, 113.1 ppm. ESI$^+$ MS: *m/z* 224 ({M + H}$^+$, 100%), 246 ({M + Na}$^+$, 25%).

L7: 4-Methylpyrazole (0.57 mL, 0.56 g, 6.8 mmol, Acros), ^{t}BuOK (0.77 g, 6.9 mmol), and 6-chloro-4,4'-dimethyl-2,2'-bipyridine [49] (1 g, 4.6 mmol) gave white solid: 1.09 g (4.1 mmol, 89%). *Anal.* Calc. for $C_{16}H_{16}N_4$ (MW 264.33): C, 72.70; H, 6.10; N, 21.20. Found: C, 73.08; H, 6.25; N, 21.59%. ^{1}H NMR (400 MHz, $CDCl_3$): δ = 8.56 (d, *J* = 4.8 Hz, 1H), 8.52 (s, 1H), 8.28 (s, 1H), 8.13 (s, 1H), 7.81 (s, 1H), 7.58 (s, 1H), 7.18 (d, *J* = 4.4 Hz, 1H), 2.50 (s, 6H, CH_3), 2.22 (s, 3H, CH_3) ppm. ^{13}C NMR (100 MHz, $CDCl_3$): δ = 155.6, 154.5, 151.4, 151.3, 149.1, 148.2, 143.0, 125.8, 125.0, 122.2, 119.5, 118.3, 112.6, 21.6, 21.5, 9.3 ppm. ESI$^+$ MS: *m/z* 265 ($\{M + H\}^+$, 100%).

L8: 3,5-Dimethylpyrazole (0.66 g, 6.9 mmol, Fluka), ^{t}BuOK (0.77 g, 6.9 mmol), and 6-chloro-4,4'-dimethyl-2,2'-bipyridine [49] (1 g, 4.6 mmol) gave pale yellow solid: 0.876 g (3.1 mmol, 68%). *Anal.* Calc. for $C_{17}H_{18}N_4$ (MW 278.35): C, 73.35; H, 6.52; N, 20.13. Found: C, 73.25; H, 6.64; N, 20.66%. ^{1}H NMR (400 MHz, CD_2Cl_2): δ = 8.54 (d, *J* = 4.8 Hz, 1H), 8.22 (s, br, 2H), 7.76 (s, 1H), 7.21 (s, br, 1H), 6.07 (s, 1H), 2.80 (s, 3H, CH_3), 2.52 (s, 3H, CH_3), 2.47 (s, 3H, CH_3), 2.30 (s, 3H, CH_3) ppm. ^{1}H NMR (400 MHz, $CDCl_3$): δ = 8.58 (s, 1H), 8.23 (s, br, 2H), 7.77 (s, 1H), 7.23 (br, 1H), 6.05 (s, 1H), 2.78 (s, 3H, CH_3), 2.51 (s, 6H, CH_3), 2.34 (s, 3H, CH_3) ppm. ^{13}C NMR (100 MHz, $CDCl_3$): δ = 155.9, 154.2, 153.2, 151.0, 149.8, 149.1, 148.2, 141.5, 124.9, 122.3, 119.2, 116.4, 109.2, 21.63, 21.57, 15.2, 13.9 ppm. ESI$^+$ MS: *m/z* 279 ($\{M + H\}^+$, 100%).

L9: 1,2,4-Triazole (0.47 g, 6.8 mmol, Aldrich), ^{t}BuOK (0.77 g, 6.9 mmol, Acros), and 6-chloro-4,4'-dimethyl-2,2'-bipyridine [49] (1 g, 4.6 mmol) gave pale pink solid: 0.39 g (1.6 mmol, 34%). The reaction did not went to completion: 6-chloro-4,4'-dimethyl-2,2'-bipyridine was still present in the reaction mixture when the reaction was terminated. *Anal.* Calc. for $C_{14}H_{13}N_5$ (MW 251.29): C, 66.92; H, 5.21; N, 27.87. Found: C, 66.68; H, 5.28; N, 27.98%. ^{1}H NMR (400 MHz, CD_2Cl_2): δ = 9.35 (s, 1H), 8.56 (d, *J* = 4.8 Hz, 1H), 8.33 (s, 1H), 8.31 (s, 1H), 8.11 (s, 1H), 7.79 (s, 1H), 7.23 (d, *J* = 4.4 Hz, 1H), 2.57 (s, 3H, CH_3), 2.50 (s, 3H, CH_3) ppm. ^{1}H NMR (400 MHz, $CDCl_3$): δ = 9.41 (s, br, 1H), 8.65 (s, br, 1H), 8.35 (s, br, 1H), 8.29 (s, 1H), 8.14 (s, 1H), 7.82 (s, 1H), 1H obscured by solvent signal, 2.58 (s, 6H, CH_3) ppm. ^{13}C NMR (100 MHz, $CDCl_3$): δ = 155.0, 154.7, 152.9, 152.2, 149.2, 149.1, 148.4, 141.7, 125.4, 122.2, 121.3, 113.6, 21.6, 21.5 ppm. ESI$^+$ MS: *m/z* 252 ($\{M + H\}^+$, 100%), 274 ($\{M + Na\}^+$, 5%).

4.2. Synthesis of cobalt(II) complexes

The structures of **1**–**9** are shown in Scheme 1. The reactions were performed under argon. The solvents were neither deoxygenated nor dried. The ligand (small excess) was dissolved in methanol (5 mL) at 60 °C. Solid $CoCl_2{\cdot}6H_2O$ (Fluka) was added to this solution. The colour of the solution changed immediately from colourless to red. The ligand **L7** on its own is not soluble in methanol; however, addition of $CoCl_2{\cdot}6H_2O$ gives a solution of the complex. For complexes **3** and **6**, the solution shortly after mixing (5–10 min) turned into a suspension; therefore, water (0.5–1 mL) was added to dissolve the precipitate. Reaction mixture was stirred at 60°C for 90 min to give pink (**1**) or red (**2**–**9**) solution. The solution was cooled to RT. It was added drop-wise to a stirred solution of KPF_6 (1–1.3 g, 5.4–7.1 mmol, large excess) in 30 mL of water, in order to convert the complex to hexafluorophosphate salt. The precipitate immediately formed. The suspension was stirred at RT for 30 min. The solid was filtered; washed with water (to remove inorganic salts) and ether (to remove free ligand); and dried under vacuum. **1**–**9** are moisture- and air-stable solids. Complexes **3**, **6**, and **9** are insoluble in dichloromethane. All of the observed ^{1}H NMR signals of **1**–**9** were singlets (information on *J*-coupling is lost); integration of the signals was often not informative. Further details are provided below.

1: $CoCl_2{\cdot}6H_2O$ (150 mg, 0.63 mmol) and **L1** (350 mg, 2.02 mmol) gave pale yellow-pink solid: 507 mg (0.58 mmol, 93%). *Anal.* Calc. for $C_{30}H_{33}CoF_{12}N_9P_2$ (MW 868.51): C, 41.49; H, 3.83; N, 14.51. Found: C, 41.77; H, 3.97; N, 14.65%. ^{1}H NMR spectrum (400 MHz, CD_3CN or acetone-d_6) was not informative. ^{19}F NMR (376 MHz, acetone-d_6): $\delta = -72.0$ (d, $J_{P–F}$ = 707 Hz, 6F, PF_6) ppm. ESI$^+$ TOF MS: *m/z* 289.0 ($\{M - 2PF_6\}^{2+}$, 90%), 550.0 ($\{M - L - PF_6\}^{+}$, 5%).

2: $CoCl_2·6H_2O$ (150 mg, 0.63 mmol) and **L2** (349 mg, 2.0 mmol) gave pale pink solid: 483 mg (0.56 mmol, 88%). *Anal.* Calc. for $C_{30}H_{33}CoF_{12}N_9P_2$ (MW 868.51): C, 41.49; H, 3.83; N, 14.51. Found: C, 41.68; H, 3.71; N, 14.54%. ^1H NMR spectrum (400 MHz, CD_3CN or acetone-d_6) was not informative. ^{19}F NMR (376 MHz, acetone-d_6): δ = −72.1 (d, $J_{P–F}$ = 707 Hz, 6F, PF_6) ppm. ESI$^+$ TOF MS: *m/z* 289.1 ($\{M – 2PF_6\}^{2+}$).

3: $CoCl_2·6H_2O$ (150 mg, 0.63 mmol) and **L3** (317 mg, 1.3 mmol) gave pale brownish-yellow solid: 343 mg (0.41 mmol, 66%). *Anal.* Calc. for $C_{26}H_{26}CoF_{12}N_{10}P_2$ (MW 827.41): C, 37.74; H, 3.17; N, 16.93. Found: C, 37.87; H, 3.25; N, 16.96%. ^1H NMR (400 MHz, CD_3CN): δ = 75.0, 61.0, 56.3, 14.3, 8.2 (CH_3) ppm. ^1H NMR (400 MHz, acetone-d_6): δ = 74.7, 61.7, 56.8, 14.1, 8.3 (CH_3) ppm. ^{19}F NMR (376 MHz, acetone-d_6): δ = −72.08 (d, $J_{P–F}$ = 707 Hz, 6F, PF_6) ppm. ESI$^+$ TOF MS: *m/z* 682.1 ($\{M – PF_6\}^+$).

4: $CoCl_2·6H_2O$ (150 mg, 0.63 mmol) and **L4** (313 mg, 1.3 mmol) gave pale brownish-yellow solid: 397 mg (0.48 mmol, 77%). *Anal.* Calc. for $C_{28}H_{24}CoF_{12}N_8P_2$ (MW 821.41): C, 40.94; H, 2.95; N, 13.64. Found: C, 40.83; H, 3.06; N, 13.78%. ^1H NMR (400 MHz, CD_3CN): δ = 110.1, 94.3, 91.2, 75.2, 70.8, 43.2, 38.9, 19.1, 14.6, 3.1 (CH_3) ppm. ^1H NMR (400 MHz, acetone-d_6): δ = 109.8 (2H), 94.6 (2H), 91.5 (2H), 75.3 (2H), 71.0 (2H), 43.3 (2H), 39.4 (2H), 19.3 (2H), 14.8 (2H), 3.1 (6H, CH_3) ppm. ^{19}F NMR (376 MHz, acetone-d_6): δ = −71.7 (d, $J_{P–F}$ = 707 Hz, 6F, PF_6) ppm. ESI$^+$ TOF MS: *m/z* 676.1 ($\{M – PF_6\}^+$).

5: $CoCl_2·6H_2O$ (150 mg, 0.63 mmol) and **L5** (331 mg, 1.3 mmol) gave pale brown solid: 464 mg (0.55 mmol, 87%). *Anal.* Calc. for $C_{30}H_{28}CoF_{12}N_8P_2$ (MW 849.46): C, 42.42; H, 3.32; N, 13.19. Found: C, 42.13; H, 3.33; N, 13.29%. ^1H NMR (400 MHz, CD_3CN): one set of aromatic H was not found at 135 ppm to −50 ppm; δ = 83.1, 78.0, 77.2, 71.0, 51.2, 15.8, 12.7, 7.2, −2.1 ppm. ^1H NMR (400 MHz, acetone-d_6): one set of aromatic H was not found at 135 ppm to −50 ppm; δ = 83.1 (2H), 78.2 (2H), 78.1 (2H), 72.0 (2H), 51.1 (2H), 15.9 (6H, CH_3), 12.9 (2H), 7.8 (2H), −0.1 (6H, CH_3) ppm. ^{19}F NMR (376 MHz, acetone-d_6): δ = −71.9

(d, $J_{P–F}$ = 707 Hz, 6F, PF_6) ppm. ESI^+ TOF MS: *m/z* 704.1 ($\{M – PF_6\}^+$, 100%), 279.6 ($\{M – 2PF_6\}^{2+}$, 90%).

6: $CoCl_2{\cdot}6H_20$ (120 mg, 0.50 mmol) and **L6** (236 mg, 1.06 mmol) gave pale pink-yellow solid: 301 mg (0.38 mmol, 76%). *Anal.* Calc. for $C_{24}H_{18}CoF_{12}N_{10}P_2$ (MW 795.33): C, 36.24; H, 2.28; N, 17.61. Found: C, 36.05; H, 2.35; N, 17.82%. ^1H NMR (400 MHz, CD_3CN): δ = 118.8, 96.7, 93.0, 77.9, 43.4, 32.0, 20.3, 17.1, 12.3 ppm. ^{19}F NMR (376 MHz, CD_3CN): δ = −72.8 (d, $J_{P–F}$ = 705 Hz, 6F, PF_6) ppm. ^1H NMR (400 MHz, acetone-d_6): δ = 118.5, 96.7, 93.9, 78.6, 43.2, 31.8, 20.8, 17.8, 12.4 ppm. ^{19}F NMR (376 MHz, acetone-d_6): δ = −72.2 (d, $J_{P–F}$ = 707 Hz, 6F, PF_6) ppm.

7: $CoCl_2{\cdot}6H_20$ (120 mg, 0.50 mmol) and **L7** (280 mg, 1.06 mmol) gave pale brown solid: 248 mg (0.28 mmol, 57%). *Anal.* Calc. for $C_{32}H_{32}CoF_{12}N_8P_2$ (MW 877.51): C, 43.80; H, 3.68; N, 12.77. Found: C, 44.03; H, 3.43; N, 13.13%. ^1H NMR (400 MHz, CD_3CN): only 6 out of 7 expected sets of aromatic signals were found; δ = 113.8, 91.5, 77.9, 65.9, 43.9, 41.1, 8.0 (CH_3), 2.8 (CH_3), −2.2 (CH_3) ppm. ^{19}F NMR (376 MHz, CD_3CN): δ = −72.6 (d, $J_{P–F}$ = 706 Hz, 6F, PF_6) ppm. ^1H NMR (400 MHz, acetone-d_6): δ = 112.1, 92.1, 91.5, 77.0, 67.1, 43.4, 41.0, 7.4 (CH_3), 2.7 (CH_3), −2.3 (CH_3) ppm. ^{19}F NMR (376 MHz, acetone-d_6): δ = −71.6 (d, $J_{P–F}$ = 707 Hz, 6F, PF_6) ppm. ESI^+ TOF MS: *m/z* 293.6 ($\{M – 2PF_6\}^{2+}$, 20%).

8: $CoCl_2{\cdot}6H_20$ (120 mg, 0.50 mmol) and **L8** (295 mg, 1.06 mmol) gave pale pinkish-yellow solid: 439 mg (0.48 mmol, 97%). *Anal.* Calc. for $C_{34}H_{36}CoF_{12}N_8P_2$ (MW 905.57): C, 45.09; H, 4.01; N, 12.37. Found: C, 45.13; H, 3.98; N, 12.63%. ^1H NMR (400 MHz, CD_3CN): only 5 out of 6 expected sets of aromatic signals were found; δ = 83.2, 80.5, 73.5, 70.3, 49.2, 15.6 (CH_3), 2.1 (CH_3), −1.2 (CH_3), −9.3 (CH_3) ppm. ^{19}F NMR (376 MHz, CD_3CN): δ = −72.8 (d, $J_{P–F}$ = 705 Hz, 6F, PF_6) ppm. ^1H NMR (400 MHz, acetone-d_6): only 5 out of 6 expected sets of aromatic signals were found; δ = 83.2, 80.2, 74.5, 70.9, 49.0, 15.6 (CH_3), 1.9 (CH_3),

−1.2 (CH_3), −7.4 (CH_3) ppm. ^{19}F NMR (376 MHz, acetone-d_6): $\delta = -71.9$ (d, $J_{\mathrm{P-F}} = 707$ Hz, 6F, PF_6) ppm. ESI$^+$ TOF MS: *m/z* 760.2 ($\{M - PF_6\}^+$, 5%), 307.6 ($\{M - 2PF_6\}^{2+}$, 100%).

9: $CoCl_2{\cdot}6H_20$ (90 mg, 0.38 mmol) and **L9** (200 mg, 0.80 mmol) gave pale pink solid: 271 mg (0.32 mmol, 84%). *Anal.* Calc. for $C_{28}H_{26}CoF_{12}N_{10}P_2$ (MW 851.44): C, 39.50; H, 3.08; N, 16.45. Found: C, 39.45; H, 2.86; N, 16.46%. ^{1}H NMR (400 MHz, CD_3CN): δ = 123.4, 92.2, 91.7, 80.1, 41.3, 26.8, 21.4, 10.6 (CH_3), −1.3 (CH_3) ppm. ^{19}F NMR (376 MHz, CD_3CN): $\delta = -72.7$ (d, $J_{\mathrm{P-F}} = 705$ Hz, 6F, PF_6) ppm. ^{1}H NMR (400 MHz, acetone-d_6): δ = 122.3, 92.5, 92.3, 80.1, 41.1, 27.2, 21.6, 10.6 (CH_3), −1.4 (CH_3) ppm. ^{19}F NMR (376 MHz, acetone-d_6): $\delta = -71.8$ (d, $J_{\mathrm{P-F}} = 707$ Hz, 6F, PF_6) ppm.

4.3. Electrochemistry

Electrochemical experiments were conducted in DMF (99.8%, Extra Dry, over Molecular Sieves, AcroSeal®, Acros) or acetonitrile (99.9%, Extra Dry, over Molecular Sieves, AcroSeal®, Acros), with 0.1 M tetra-*n*-butylammonium hexafluorophosphate (Fluka, electrochemical grade) as the supporting electrolyte, with a PC controlled AutoLab PSTAT10 electrochemical workstation.

The experiments were carried out under argon in an electrochemical cell through which a stream of Ar was passed (the flow of Ar was stopped during the measurement to prevent stirring of the solution). Gold disk or glassy-carbon disk (3 mm diameter), platinum spiral, and platinum wire served as working, counter, and quasi-reference electrodes. To clean, the working electrodes were polished on a pad in ethanol slurry of abrasive paste (Metrohm), briefly sonicated in ethanol, and rinsed with ethanol. At the end of each experiment, ferrocene was added as an internal reference [44]. Estimated error: ±50 mV. Cyclic voltammetry was performed at scan rates of 10–0.05 V/s. Peak-to-peak separation for the ferrocene couple (reference) in acetonitrile was 83–107 mV at 1 V/s and 68–82 mV at 0.1 V/s [44].

Acknowledgements

European Union (FP7-ENERGY-2010-FET, MOLESOL, Ref.: 256617, http://www.molesol.eu/). MKN acknowledges the World Class University program (Photovoltaic Materials, Department of Material Chemistry, Korea University) funded by the Ministry of Education, Science and Technology through the National Research Foundation of Korea (Ref.: R31-2008-000-10035-0).

Appendix A. Supplementary material

Redox properties (Tables S1 and S2; Fig. S1–S6); absorption spectra (Table S3; Fig. S7–S24); NMR spectra. Supplementary data associated with this article can be found, in the online version, at http://dx.doi.org/...

References

[1] (a) N. Tanaka, Y. Sato, Bull. Chem. Soc. Jpn. 41 (1968) 2059; (b) S. Margel, W. Smith, F.C. Anson, J. Electrochem. Soc. 125 (1978) 241.

[2] G. Arena, R.P. Bonomo, S. Musumeci, E. Rizzarelli, Z. anorg. allg. Chem. 412 (1975) 161.

[3] R.K. Boggess, D.A. Zatko, Inorg. Chem. 15 (1976) 626.

[4] B.C. Willett, F.C. Anson, J. Electrochem. Soc. 129 (1982) 1260.

[5] D.J. Szalda, C. Creutz, D. Mahajan, N. Sutin, Inorg. Chem. 22 (1983) 2372.

[6] K.R. Adam, P.A. Anderson, T. Astley, I.M. Atkinson, J.M. Charnock, C.D. Garner, J.M. Gulbis, T.W. Hambley, M.A. Hitchman, F.R. Keene, E.R.T. Tiekink, J. Chem. Soc., Dalton Trans. (1997) 519.

[7] (a) E.A. Medlycott, I. Theobald, G.S. Hanan, Eur. J. Inorg. Chem. (2005) 1223; (b) M.G.B. Drew, M.R.St.J. Foreman, A. Geist, M.J. Hudson, F. Marken, V. Norman, M. Weigl, Polyhedron 25 (2006) 888.

[8] D. Chen, P.-L. Fabre, O. Reynes, Electrochim. Acta 56 (2011) 8603.

[9] (a) C.M. Araujo, M.D. Doherty, S.J. Konezny, O.R. Luca, A. Usyatinsky, H. Grade, E. Lobkovsky, G.L. Soloveichik, R.H. Crabtree, V.S. Batista, Dalton Trans. 41 (2012) 3562; (b) L.J.K. Cook, F. Tuna, M.A. Halcrow, Dalton Trans. 42 (2013) 2254.

[10] R.S. Gaddie, C.B. Moss, C.M. Elliott, Langmuir 29 (2013) 825.

[11] (a) S. Losse, J.G. Vos, S. Rau, Coord. Chem. Rev. 254 (2010) 2492; (b) V. Artero, M. Chavarot-Kerlidou, M. Fontecave, Angew. Chem. Int. Ed. 50 (2011) 7238.

[12] A.R. Guadalupe, D.A. Usifer, K.T. Potts, H.C. Hurrell, A.-E. Mogstad, H.D. Abruña, J. Am. Chem. Soc. 110 (1988) 3462.

[13] H.C. Hurrell, A.-L. Mogstad, D.A. Usifer, K.T. Potts, H.D. Abruña, Inorg. Chem. 28 (1989) 1080.

[14] (a) K.-M. Lam, K.-Y. Wong, S.-M. Yang, C.-M. Che, J. Chem. Soc., Dalton Trans. (1995) 1103; (b) J.P. Bigi, T.E. Hanna, W.H. Harman, A. Chang, C.J. Chang, Chem. Commun. 46 (2010) 958; (c) C.-F. Leung, S.-M. Ng, C.-C. Ko, W.-L. Man, J. Wu, L. Chen, T.-C. Lau, Energy Environ. Sci. 5 (2012) 7903.

[15] (a) D.J. Wasylenko, C. Ganesamoorthy, J. Borau-Garcia, C.P. Berlinguette, Chem. Commun. 47 (2011) 4249; (b) Y. Sun, J. Sun, J.R. Long, P. Yang, C.J. Chang, Chem. Sci. 4 (2013) 118.

[16] H. Nusbaumer, J.-E. Moser, S.M. Zakeeruddin, Md.K. Nazeeruddin, M. Grätzel, J. Phys. Chem. B 105 (2001) 10461.

[17] S.A. Sapp, C.M. Elliott, C. Contado, S. Caramori, C.A. Bignozzi, J. Am. Chem. Soc., 124 (2002) 11215.

[18] (a) S.M. Feldt, E.A. Gibson, E. Gabrielsson, L. Sun, G. Boschloo, A. Hagfeldt, J. Am. Chem. Soc. 132 (2010) 16714; (b) K. Miettunen, T. Saukkonen, X. Li, C.H. Law, Y.K. Sheng, J. Halme, A. Tiihonen, P.R.F. Barnes, T. Ghaddar, I. Asghar, P. Lund, B.C. O’Regan, J. Electrochem. Soc. 160 (2013) H132.

[19] S. Ahmad, T. Bessho, F. Kessler, E. Baranoff, J. Frey, C. Yi, M. Grätzel, Md.K. Nazeeruddin, Phys. Chem. Chem. Phys. 14 (2012) 10631.

[20] E. Mosconi, J.-H. Yum, F. Kessler, C.J.G. García, C. Zuccaccia, A. Cinti, Md.K. Nazeeruddin, M. Grätzel, F. De Angelis, J. Am. Chem. Soc. 134 (2012) 19438.

[21] J. Burschka, A. Dualeh, F. Kessler, E. Baranoff, N.-L. Cevey-Ha, C. Yi, Md.K. Nazeeruddin, M. Grätzel, J. Am. Chem. Soc. 133 (2011) 18042.

[22] Y.-W.D. Chen, K.S.V. Santhanam, A.J. Bard, J. Electrochem. Soc. 129 (1982) 61.

[23] P.J. Steel, F. LaHousse, D. Lerner, C. Marzin, Inorg. Chem. 22 (1983) 1488.

[24] (a) A.T. Baker, N.J. Ferguson, H.A. Goodwin, Aust. J. Chem. 37 (1984) 2421; (b) A.S. Abushamleh, H.A. Goodwin, Aust. J. Chem. 41 (1988) 873; (c) A.T. Baker, J.P. Matthews, Aust. J. Chem. 52 (1999) 339.

[25] D.L. Jameson, J.K. Blaho, K.T. Kruger, K.A. Goldsby, Inorg. Chem. 28 (1989) 4312.

[26] P.J. Steel, E.C. Constable, J. Chem. Soc., Dalton Trans. (1990) 1389.

[27] (a) V.J. Catalano, R. Kurtaran, R.A. Heck, A. Öhman, M.G. Hill, Inorg. Chim. Acta 286 (1999) 181; (b) Q.-H. Wei, S.P. Argent, H. Adams, M.D. Ward, New J. Chem. 32 (2008) 73; (c) F. Schramm, R. Chandrasekar, T.A. Zevaco, M. Rudolph, H. Görls, W. Poppitz, M. Ruben, Eur. J. Inorg. Chem. (2009) 53.

[28] T. Ayers, R. Turk, C. Lane, J. Goins, D. Jameson, S.J. Slattery, Inorg. Chim. Acta 357 (2004) 202.

[29] D. Girnt, P.W. Roesky, A. Geist, C.M. Ruff, P.J. Panak, M.A. Denecke, Inorg. Chem. 49 (2010) 9627.

[30] (a) S. Develay, O. Blackburn, A.L. Thompson, J.A.G. Williams, Inorg. Chem. 47 (2008) 11129; (b) T. Hajra, J.K. Bera, V. Chandrasekhar, Inorg. Chim. Acta 372 (2011) 53; (c) D. Sykes, I.S. Tidmarsh, A. Barbieri, I.V. Sazanovich, J.A. Weinstein, M.D. Ward, Inorg. Chem. 50 (2011) 11323.

[31] N.M. Shavaleev, R. Scopelliti, M. Grätzel, Md.K. Nazeeruddin, Inorg. Chim. Acta 404 (2013) 210.

[32] D.L. Jameson, K.A. Goldsby, J. Org. Chem. 55 (1990) 4992.

[33] (a) M.A.M. Garcia, A. Gelling, D.R. Noble, K.G. Orrell, A.G. Osborne, V. Šik, Polyhedron 15 (1996) 371. (b) C. Carbonera, J.S. Costa, V.A. Money, J. Elhaïk, J.A.K. Howard, M.A. Halcrow, J.-F. Létard, Dalton Trans. (2006) 3058.

[34] A. Gelling, K.G. Orrell, A.G. Osborne, V. Šik, J. Chem. Soc., Dalton Trans. (1994) 3545.

[35] A.J. Downard, G.E. Honey, P.J. Steel, Inorg. Chem. 30 (1991) 3733.

[36] (a) A.F. Williams, C. Piguet, G. Bernardinelli, Angew. Chem. Int. Ed. 30 (1991) 1490; (b) L.J. Charbonnière, A.F. Williams, C. Piguet, G. Bernardinelli, E. Rivara-Minten, Chem. Eur. J. 4 (1998) 485.

[37] (a) T. Astley, A.J. Canty, M.A. Hitchman, G.L. Rowbottom, B.W. Skelton, A.H. White, J. Chem. Soc., Dalton Trans. (1991) 1981; (b) T. Astley, J.M. Gulbis, M.A. Hitchman, E.R.T. Tiekink, J. Chem. Soc., Dalton Trans. (1993) 509.

[38] T. Ayers, S. Scott, J. Goins, N. Caylor, D. Hathcock, S. J. Slattery, D.L. Jameson, Inorg. Chim. Acta 307 (2000) 7.

[39] (a) N. Saha, S.K. Kar, J. Inorg. Nucl. Chem. 39 (1977) 1236; (b) G. Dong, J.P. Matthews, D.C. Craig, A.T. Baker, Inorg. Chim. Acta 284 (1999) 266; (c) J.M. Holland, C.A. Kilner, M. Thornton-Pett, M.A. Halcrow, Polyhedron 20 (2001) 2829; (d) C. Arici, D. Ülkü, R. Kurtaran, K.C. Emregül, O. Atakol, Z. Kristallogr. 218 (2003) 497; (e) A.R. Karam, E.L. Catarí, F. López-Linares, G. Agrifoglio, C.L. Albano, A. Díaz-Barrios, T.E. Lehmann, S.V. Pekerar, L.A. Albornoz, R. Atencio, T. González, H.B. Ortega, P. Joskowics, Appl. Catal. A 280 (2005) 165; (f) C. Hopa, R. Kurtaran, M. Alkan, H. Kara, R. Hughes, Trans. Met. Chem. 35 (2010) 1013; (g) D. Gong, X. Jia, B. Wang, X. Zhang, L. Jiang, J. Organomet. Chem. 702 (2012) 10.

[40] X. Ren, B.D. Alleyne, P.I. Djurovich, C. Adachi, I. Tsyba, R. Bau, M.E. Thompson, Inorg. Chem. 43 (2004) 1697.

[41] X.-j. Wang, J. Tan, K. Grozinger, R. Betageri, T. Kirrane, J.R. Proudfoot, Tetrahedron Lett. 41 (2000) 5321.

[42] J.S. Judge, W.A. Baker, Jr., Inorg. Chim. Acta 1 (1967) 68.

[43] (a) P. Ellis, R.G. Wilkins, J. Chem. Soc. (1959) 299; (b) B. Brisig, E.C. Constable, C.E. Housecroft, New J. Chem. 31 (2007) 1437.

[44] N.G. Tsierkezos, J. Solution Chem. 36 (2007) 289.

[45] L. Xu, X.-T. Chen, Y. Xu, D.-R. Zhu, X.-Z. You, L.-H. Weng, J. Mol. Struct. 559 (2001) 361.

[46] M. Ruben, E. Breuning, M. Barboiu, J.-P. Gisselbrecht, J.-M. Lehn, Chem. Eur. J. 9 (2003) 291.

[47] (a) N. Komatsuzaki, Y. Himeda, T. Hirose, H. Sugihara, K. Kasuga, Bull. Chem. Soc. Jpn. 72 (1999) 725; (b) J. Lombard, R. Boulaouche, D.A. Jose, J. Chauvin, M.-N. Collomb, A. Deronzier, Inorg. Chim. Acta 363 (2010) 234.

[48] Sk. Jasimuddin, T. Yamada, K. Fukuju, J. Otsuki, K. Sakai, Chem. Commun. 46 (2010) 8466.

[49] F. Wang, A.W. Schwabacher, Tetrahedron Lett. 40 (1999) 4779.

Table 1

UV-Vis absorption maxima in acetonitrile.[a]

	λ_{abs}/nm (ε/10^3 M^{-1} cm^{-1})
L1	263 (11), 282 (13)
L2	261 (14), 288 (13)
L3	214 (11), 252 (26), 277 (12), 308 (21)
L4	237 (20), 267 (19), 306 (15)
L5	236 (21), 264 (21), 303 (12)
L6	231 (19), 297 (14)
L7	243 (21), 268 (18), 289 (13), 304 (14)
L8	242 (22), 265 (19), 289 (12), 300 (12)
L9	237 (21), 295 (13)
1	259 (36), 284 (32)
2	231 (21), 261 (42), 292 (31)
3	231 (24), 254 (31), 272 (39), 316 (25), 402 (0.8)
4	237 (29), 272 (34), 323 (24)
5	236 (35), 269 (35), 326 (24)
6	225 (40), 257 (24), 312 (25)
7	209 (69), 270 (35), 317 (24)
8	208 (65), 268 (36), 320 (24)
9	213 (69), 259 (26), 309 (26)

[a] Room temperature. At 200–700 nm. Errors: ±2 nm for λ_{abs}; ±5% for ε. Absorption maxima in dichloromethane are listed in Table S3.

Table 2

Redox potentials of cobalt(II) complexes in acetonitrile.[a]

Complex	Electrode	$E_{1/2}^{\mathrm{ox}}$/V	$E_{1/2}^{\mathrm{red}}$/V		ΔE/V[b]
		Co(III/II)	Co(II/I)	L/L^{-}	
1	Gold	0.19 (130)	−1.57 (100) [c]		1.76
	GC	[d]	−1.56 (93)		
2	Gold	0.21 (110)	−1.55 (110) [c]		1.76
	GC	[d]	−1.53 (98)		
3	Gold	0.50 (93)	−1.32 (88) [c]		1.82
	GC	[d]	−1.33 (98)		
4	Gold	0.17 (100)	−1.24 (93)	−2.04 (98)	1.41
	GC	0.17 (140)	−1.24 (88)	−2.04 (98)	1.41
5	Gold	0.13 (83)	−1.25 (83)	−2.05 (88)	1.38
	GC	0.12 (110)	−1.25 (88)	−2.06 (88)	1.37
6	Gold	0.44 (180)	−1.08 (93)		1.52
	GC	0.42 (160)	−1.09 (83)		1.51
7	Gold	0.10 (88)	−1.35 (78)	−2.10 (150)	1.45
	GC	0.11 (160)	−1.34 (78)		1.45
8	Gold	0.05 (88)	−1.37 (73)	−2.14 (88)	1.42
	GC	0.05 (150)	−1.37 (78)	−2.14 (88)	1.42
9	Gold	0.37 (130)	−1.19 (93)		1.56
	GC	0.39 (350)	−1.19 (83)		1.58

[a] On gold or glassy-carbon (GC) working electrode. 0.1 M $(NBu_4)PF_6$. Scan rate: 100 mV/s. Quasi-reversible processes; $E_{1/2}^{\mathrm{red}}$ and $E_{1/2}^{\mathrm{ox}}$ are reported relative to Fc^+/Fc [44]; the anodic/cathodic peak separation is given in brackets (for the Fc^+/Fc it was 68–82 mV). Error: ±50 mV. The one-electron redox processes of **1**–**9** were assigned by comparison with the literature [1–10]. Redox potentials in DMF and at other scan rates in ACN are listed in Tables S1 and S2.

[b] Redox gap: $\Delta E = E_{1/2}^{\text{ox}}$ [Co(III/II)] − $E_{1/2}^{\text{red}}$ [Co(II/I)].

[c] Not completely reversible process.

[d] Irreversible process or wide peak-to-peak separation.

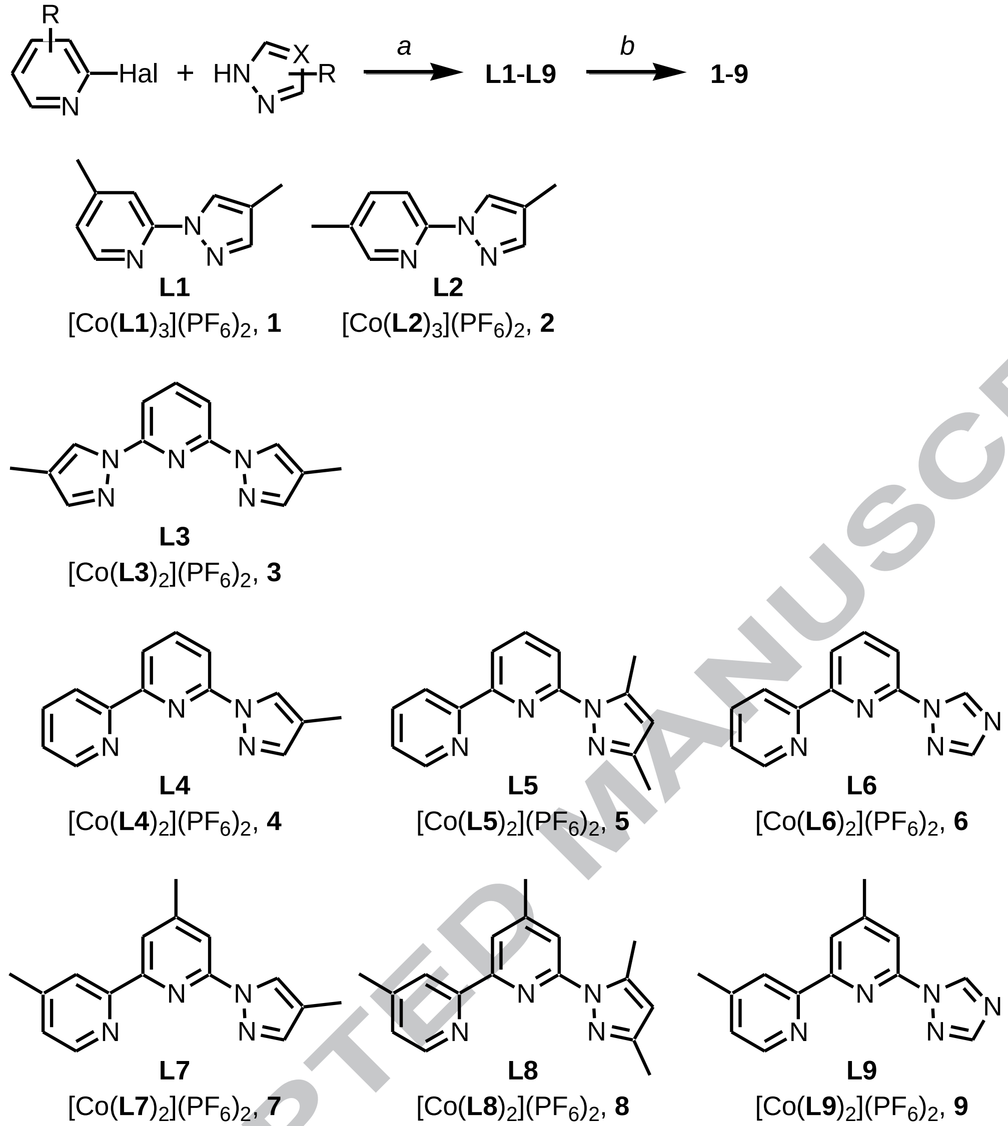

Scheme 1. Synthesis of ligands **L1**–**L9** and octahedral cobalt(II) complexes **1**–**9**: (a) ^{t}BuOK, dry DMSO, under Ar, 110–140 °C; (b) $CoCl_2{\cdot}6H_2O$ (solid), methanol, under Ar, 60 °C, KPF_6.

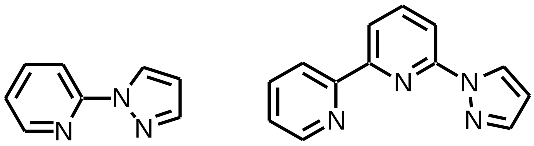

LR1
$[\mathrm{Co}(\mathbf{LR1})_3](\mathrm{PF}_6)_2$, **R1**

LR2
$[\mathrm{Co}(\mathbf{LR2})_2](\mathrm{PF}_6)_2$, **R2**

Chart 1. Reference ligands and cobalt(II) complexes [19].

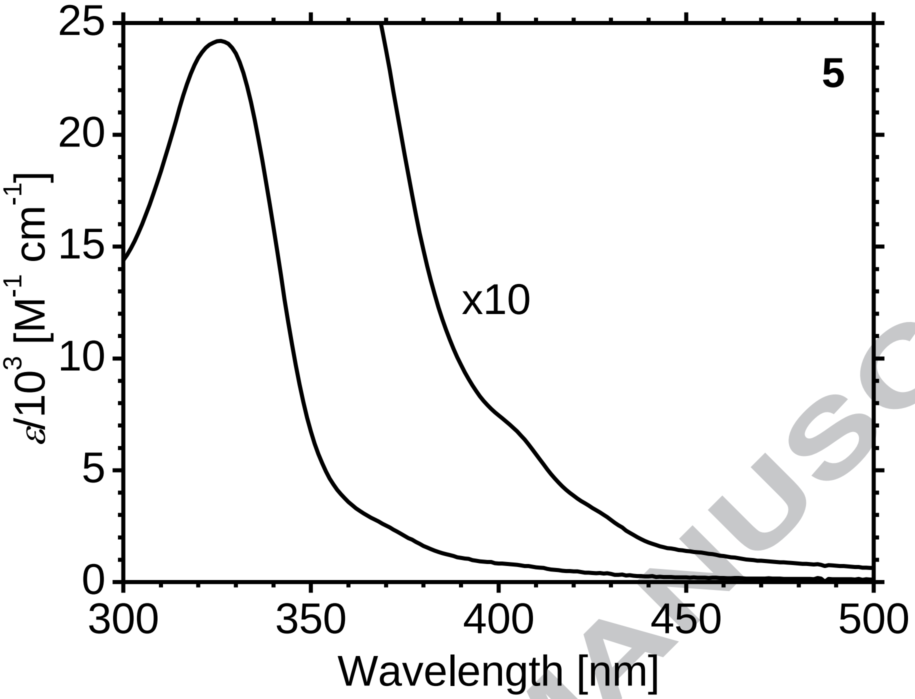

Fig. 1. Absorption spectrum of cobalt(II) complex **5** in acetonitrile (1.16×10^{-4} M). Other absorption spectra are shown in Fig. S7–S24.

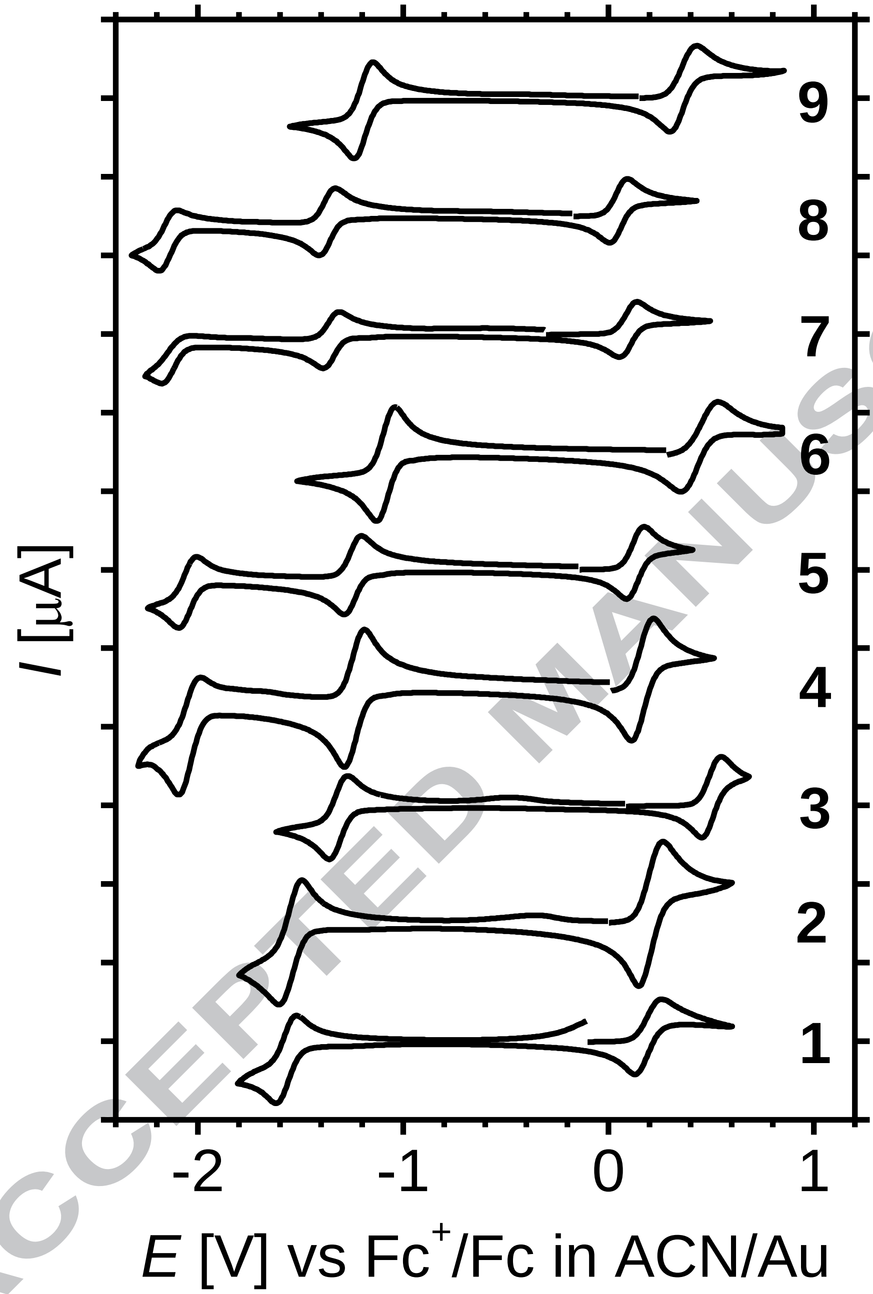

Fig. 2. Cyclic voltammograms of cobalt(II) complexes **1**–**9** on gold electrode in acetonitrile with 0.1 M NBu_4PF_6 at 100 mV/s (the first clockwise scan is shown). The unit on the vertical axis is 100 μA. CV of the Co(III/II) couple depends on the electrode history (see text). The peak at −0.8 to 0 V in the CVs of **1**–**3** is a return wave of a not completely reversible reduction.

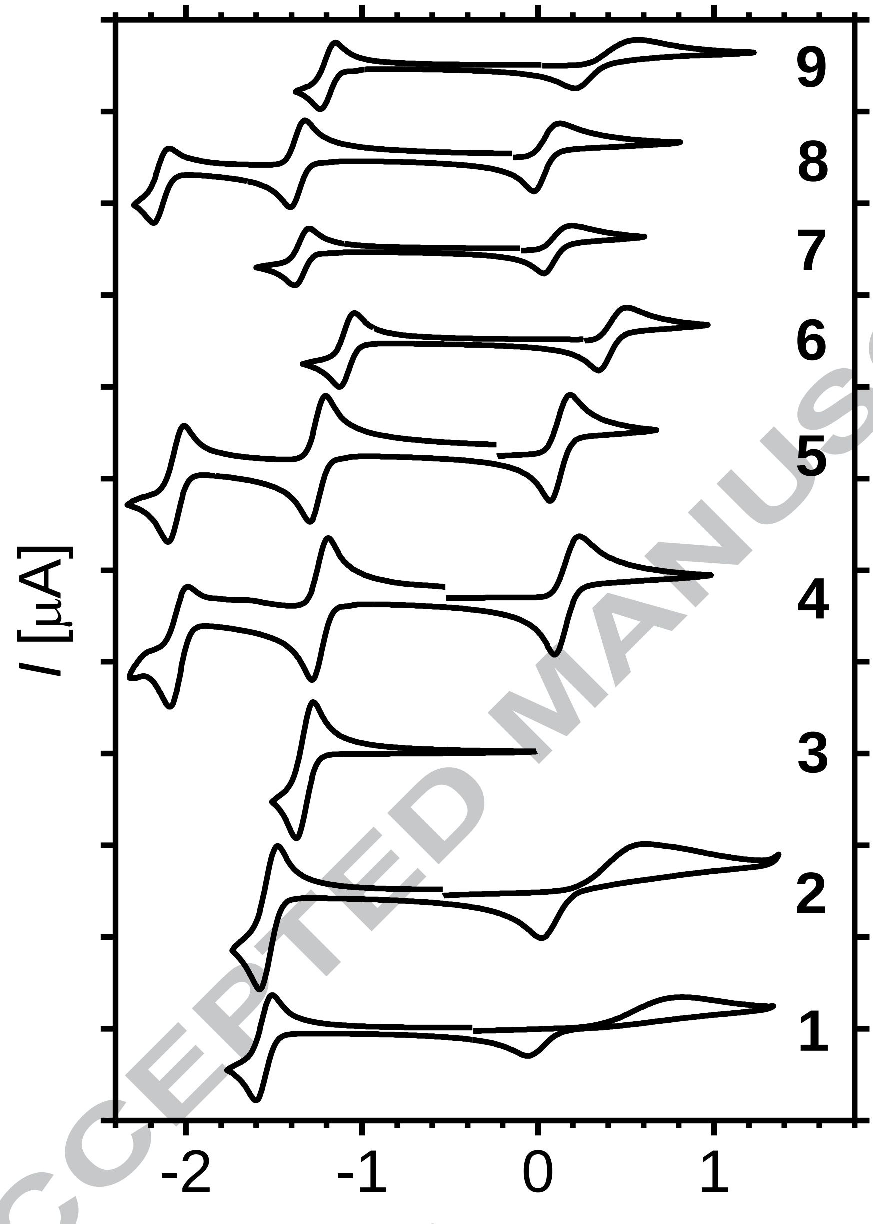

Fig. 3. Cyclic voltammograms of cobalt(II) complexes **1**–**9** on glassy-carbon electrode in acetonitrile with 0.1 M NBu_4PF_6 at 100 mV/s (the first clockwise scan is shown). The unit on the vertical axis is 100 μA. CV of the Co(III/II) couple depends on the electrode history (see text).

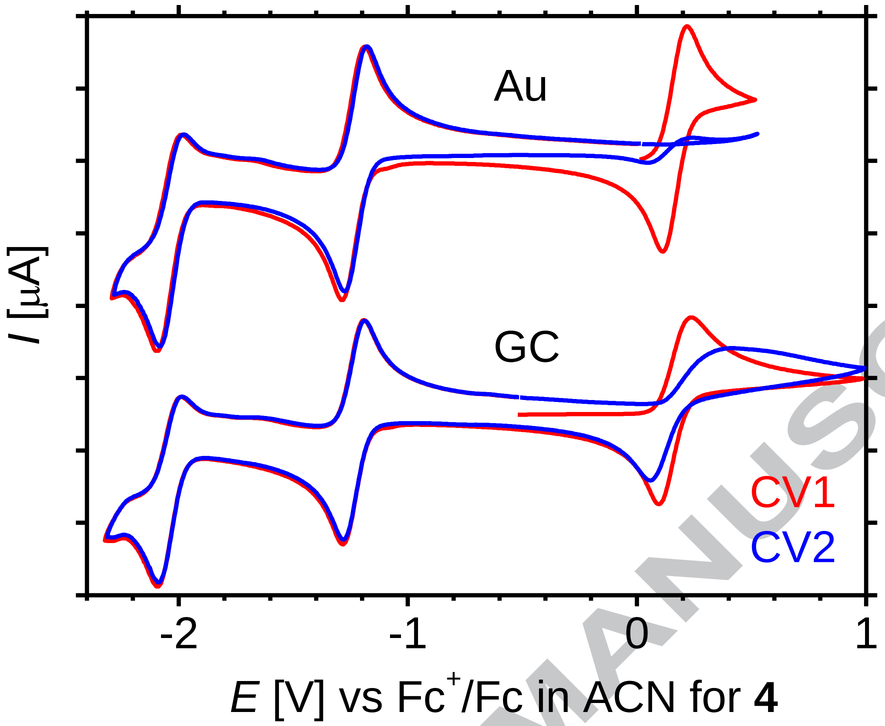

Fig. 4. Cyclic voltammograms of complex **4** on gold (Au) and on glassy-carbon (GC) electrodes in acetonitrile with 0.1 M NBu_4PF_6 at 100 mV/s; two consecutive clockwise scans are shown (CV1 and CV2). The unit on the vertical axis is 50 µA. CV of the Co(III/II) couple depends on the scan (see text); similar behavior was observed for the rest of Co(II) complexes, when DMF was used as a solvent, and at other scan rates.

Graphical Abstract

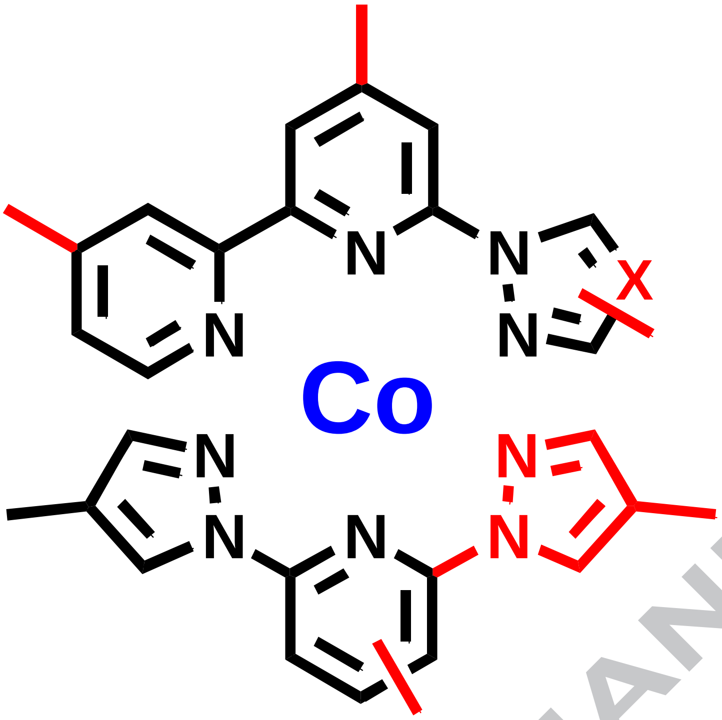

Graphical Abstract

Redox and optical properties of homoleptic octahedral cobalt(II) complexes with bidentate and tridentate azole-pyridine ligands.

Highlights

>Five new bidentate and tridentate azole-pyridine ligands.

>Nine new homoleptic octahedral cobalt(II) complexes with azole-pyridines.

>How to control redox and optical properties of cobalt(II) complexes.